Stoichiometry for drug potentiation of a pentameric ion channel

Corrie J. B. daCosta[a,1] and Steven M. Sine[a,b,1]

Departments of [a]Physiology and Biomedical Engineering, and [b]Neurology, Mayo Clinic College of Medicine, Rochester, MN 55905

Edited by Richard W. Aldrich, University of Texas at Austin, Austin, TX, and approved March 8, 2013 (received for review January 29, 2013)

Drug modulation of ion channels is a powerful means to alter physiological responses for therapeutic benefit, yet the structural bases of modulation remain poorly understood. Here we study potentiation of nicotinic α7 acetylcholine receptors, which are emerging drug targets in several neurological disorders. α7 receptors are ligand-gated ion channels composed of five identical subunits, each bearing a site for the potentiating drug PNU-120596 (PNU). How the individual subunits contribute to PNU potentiation is not known. Taking advantage of a PNU-resistant mutant, we generated receptors composed of normal and PNU-resistant subunits and tagged one of the subunits with conductance mutations to report subunit stoichiometry. We then used patch clamp recording to monitor PNU potentiation of single α7 receptors with defined stoichiometry in real time. We find that potentiation depends steeply on the number of PNU-resistant subunits and that four, and possibly five, subunits must be sensitive to PNU for potentiation to occur. Thus, by monitoring the activity of every possible subunit combination, our findings predict that at the macroscopic level, PNU potentiation is highly cooperative.

allosteric modulation | cys-loop receptor | electrical fingerprinting

Many pharmaceuticals target ion channels, which are transmembrane proteins that regulate the electrical excitability of cells (1). Most ion channels are oligomeric proteins, assembled from several homologous subunits around a central ion-conducting pore (2). This oligomeric architecture means that ion channels often contain multiple drug-binding sites, leading to a fundamental question: How many of the available drug sites are required for the action of the drug?

Pentameric ligand-gated ion channels are found in most lifeforms, ranging from bacteria to humans (3). In animals, they are the largest and most diverse family of neurotransmitter-gated ion channels, which mediate synaptic transmission throughout the nervous system (3, 4). Composed of homologous subunits, all pentameric ligand-gated ion channels are either homo- or heteropentameric. The nicotinic α7 receptor (α7) is homopentameric (5) and is one of the most abundant nicotinic acetylcholine receptors in the brain (6). α7 has been implicated in several neurodegenerative and neuropsychiatric disorders (7–9). As a result, it has emerged as a potential therapeutic target, and several α7-specific compounds have been identified (10–13). Of these, PNU-120596 (PNU) has the most pronounced effect (14). PNU itself does not trigger opening of the α7 channel but, instead, prolongs agonist-induced openings several thousand-fold, leading to a dramatic potentiation of agonist-induced responses (Fig. 1).

Previously we engineered an α7 mutant that is essentially insensitive to PNU (15). This PNU-resistant mutant functions similarly to wild-type α7 in the absence of PNU, but in the presence of PNU, it continues to exhibit only brief, unpotentiated agonist-induced channel openings (Fig. 1) (15). The mutated residues line an intrasubunit cavity framed by transmembrane α-helices. Located far from the extracellular agonist binding sites, this cavity is thought to constitute the PNU binding site (Fig. S1) (16).

Because α7 is homopentameric, receptors formed from wild-type subunits contain five intact PNU sites, whereas receptors formed from PNU-resistant subunits have all five PNU sites mutated. We therefore asked how heteropentamers, formed from combinations of these two functionally divergent subunits, would function in the presence of PNU. Specifically, how does mutating the PNU sites one at a time affect PNU potentiation?

Results

Wild-type and PNU-resistant subunits differ by only a few amino acids (15), suggesting they will coassemble to form a population in which individual receptors contain from zero to five wild-type or PNU-resistant subunits. Although the hypothesis is that the resulting heteropentameric receptors will be potentiated differently than either wild-type or mutant homopentamers, the stoichiometry of the subunits in individual heteropentamers will be unknown. What is needed is a means to directly determine the stoichiometry of wild-type and PNU-resistant subunits in individual receptors.

To determine subunit stoichiometry, we used an electrical fingerprinting strategy (17, 18) in which mutations that alter the single-channel conductance without affecting PNU potentiation (Fig. S2) are introduced into one of the two kinds of subunits. This strategy takes advantage of a structural feature inherent to eukaryotic pentameric ligand-gated ion channels: As conducting ions exit the channel's transmembrane pore, they are obliged to pass through one of five portals in the cytoplasmic domain (Fig. 2 and ref. 19). Framed by charged or polar residues from each subunit, these portals determine the single-channel conductance. In the homologous 5-HT_{3A} receptor, the presence of three arginine residues in this region is responsible for its unusually low conductance (20).

We substituted three arginine residues for anionic and polar residues that contribute to the portals in human α7 (Fig. 2*B*), and combined this subunit (wild-type α7 that has low conductance [WT_{LC}]) with the wild-type subunit (WT). Under specific conditions, patches from cells expressing only wild-type α7 subunits gave channel openings with a major Gaussian-distributed single-channel current amplitude, as well as minor components with reduced amplitudes (Fig. 2*C* and Fig. S3*A*). In subunit-mixing experiments, these minor components were avoided, as described in *Materials and Methods*. Conversely, patches from cells coexpressing both WT and WT_{LC} subunits gave channel openings with a distribution of amplitudes, which segregated into five distinguishable classes (Fig. 2*D* and Fig. S3*B*). The difference in amplitude between successive classes was regular, indicating five approximately equal contributions to single-channel conductance. Given that α7 receptors contain five equivalent subunits, a parsimonious interpretation is that the different conductance classes originate from receptors with different numbers of

Author contributions: C.J.B.D. and S.M.S. designed research; C.J.B.D. performed research; S.M.S. supervised research; C.J.B.D. analyzed data; and C.J.B.D. and S.M.S. wrote the paper.

The authors declare no conflict of interest.

This article is a PNAS Direct Submission.

[1]To whom correspondence may be addressed. E-mail: dacosta.corrie@mayo.edu or sine@mayo.edu.

This article contains supporting information online at www.pnas.org/lookup/suppl/doi:10.1073/pnas.1301909110/-/DCSupplemental.

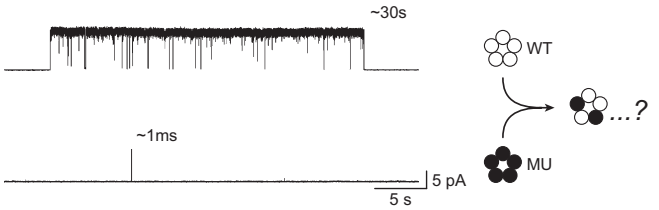

Fig. 1. Two homopentameric receptors with very different PNU potentiation. Wild-type α7 exhibits prolonged, PNU-potentiated openings in the presence of 100 μM acetylcholine and 1 μM PNU (WT; *Upper*), whereas under the same conditions, a PNU-resistant mutant exhibits brief, unpotentiated openings (MU; *Lower*). The goal of this work is to examine the potentiation of α7 heteropentamers formed by combining wild-type and PNU-resistant subunits (*Right*). Recordings were made in the cell-attached configuration with an applied voltage of −70 mV. Openings are upward deflections, and single-channel traces are filtered at 1 kHz.

incorporated low-conductance subunits (Fig. 2*E*). Thus, for each channel opening episode, the single-channel current amplitude gives an instant register of the stoichiometry of high- and low-conductance subunits.

Equipped with a means to register subunit stoichiometry, we determined the effect of PNU on α7 heteropentamers with different numbers of wild-type and PNU-resistant subunits. We began by measuring acetylcholine-elicited channel openings from cell-attached patches before and after the addition of PNU to the extracellular solution (Fig. 3). After forming a patch on a cell expressing only wild-type α7 subunits, the channel openings were initially brief, but subsequent addition of PNU led to openings that were dramatically prolonged and summed in a staircase fashion. Conversely, when the same experiment was conducted with cells expressing only PNU-resistant subunits, the agonist-induced openings were brief both before and after adding PNU. Because each patch exhibited similar activity before the addition of PNU (Fig. 3*C*), the contrasting responses to PNU reflect the divergent ability of PNU to potentiate homopentamers formed from either of the two kinds of subunits.

We then conducted the same PNU adding experiment with cells expressing both wild-type and PNU-resistant subunits, but with the PNU-resistant subunit tagged with mutations that reduce conductance. Addition of PNU produced little change in channel opening activity, mirroring patches containing receptors formed from only PNU-resistant subunits (Fig. 3*C*). Most channel openings remained brief, and thus most of the receptors were not potentiated by PNU. Because the PNU-resistant subunits have negligible conductance, and are thus electrically silent, the channel openings originated from receptors with at least a single high-conductance wild-type subunit. Furthermore, many of the channel openings exhibited large-current amplitudes corresponding to receptors containing several high-conductance wild-type subunits. Despite this, the openings were almost exclusively brief and reminiscent of receptors composed solely of PNU-resistant subunits. Qualitatively, these results show that receptors containing fewer than five wild-type α7 subunits are not potentiated by PNU.

To quantify PNU potentiation in receptors with varying subunit compositions, we acquired recordings from cell-attached patches in which both PNU and acetylcholine were continuously present within the patch pipette (Fig. 4). Recordings from patches containing receptors with only wild-type α7 subunits showed long-lived, PNU-potentiated channel openings (Fig. 4*A* and Fig. S4), whereas patches containing receptors with only mutant subunits showed brief unpotentiated openings (Fig. 4*B*). Patches containing receptors formed from the two kinds of subunits exhibited primarily brief channel openings (Fig. 4*C*), again mirroring receptors formed solely from PNU-resistant subunits. When either the wild-type α7 or the PNU-resistant subunit contained conductance-altering mutations, the channel openings exhibited variable current amplitudes (Fig. S5). As expected, these openings segregated into well-defined amplitude classes, making it possible to determine the subunit stoichiometry of individual receptors (Fig. S6).

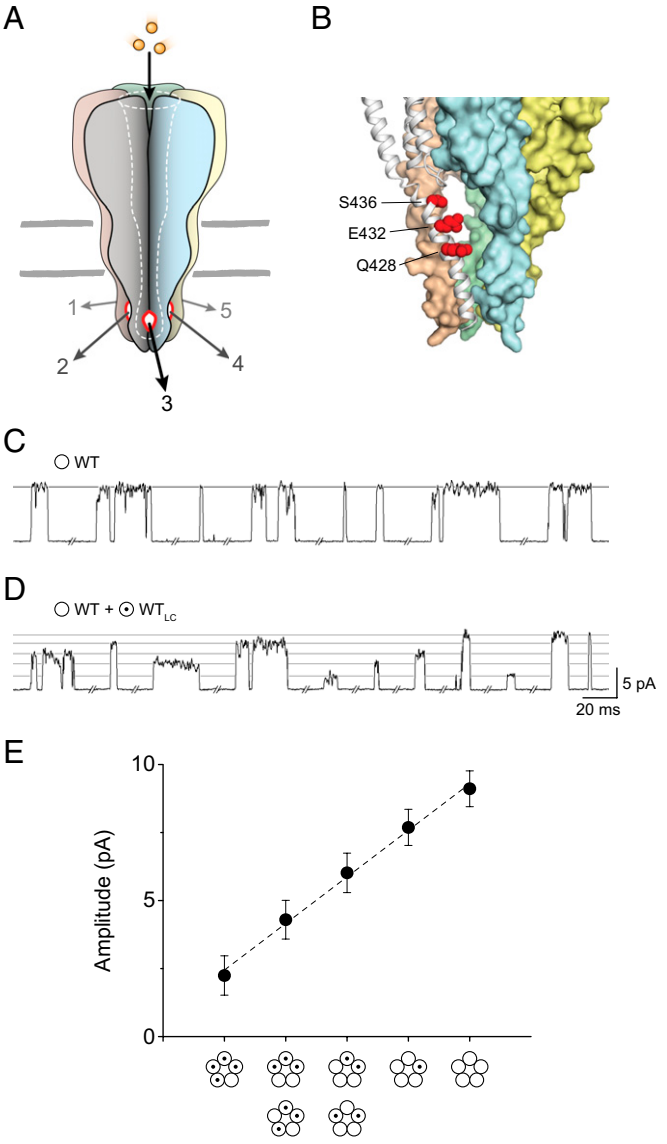

Fig. 2. Electrical fingerprinting strategy for determining subunit stoichiometry from single-channel conductance. (*A*) The cytoplasmic domain of eukaryotic pentameric ligand-gated ion channels contains five portals framed by neighboring subunits through which ions must pass to exit the channel (adapted from ref. 20). (*B*) Homology model of the α7 cytoplasmic vestibule based on the *Torpedo* acetylcholine receptor structure (Protein Data Bank ID code 2BG9, ref. 19). A single subunit is shown in gray with the side chains of residues mutated to alter single-channel conductance highlighted in red. The four other subunits are shown as surface representations. (*C* and *D*) The single-channel current amplitude of wild-type α7 channels (WT; white circles) is uniform, whereas channels incorporating subunits with conductance-altering mutations (WT$_{LC}$; white circles with dot) segregate into five amplitude classes. Openings in each were from single recordings acquired in the presence of 100 μM acetylcholine and 0.3 μM PNU. Recordings were made in the cell-attached configuration with an applied voltage of −70 mV. Traces were filtered at 1 kHz. (*E*) Single-channel amplitude is directly related to the number of incorporated low-conductance subunits. Error bars represent ± SDs about the mean.

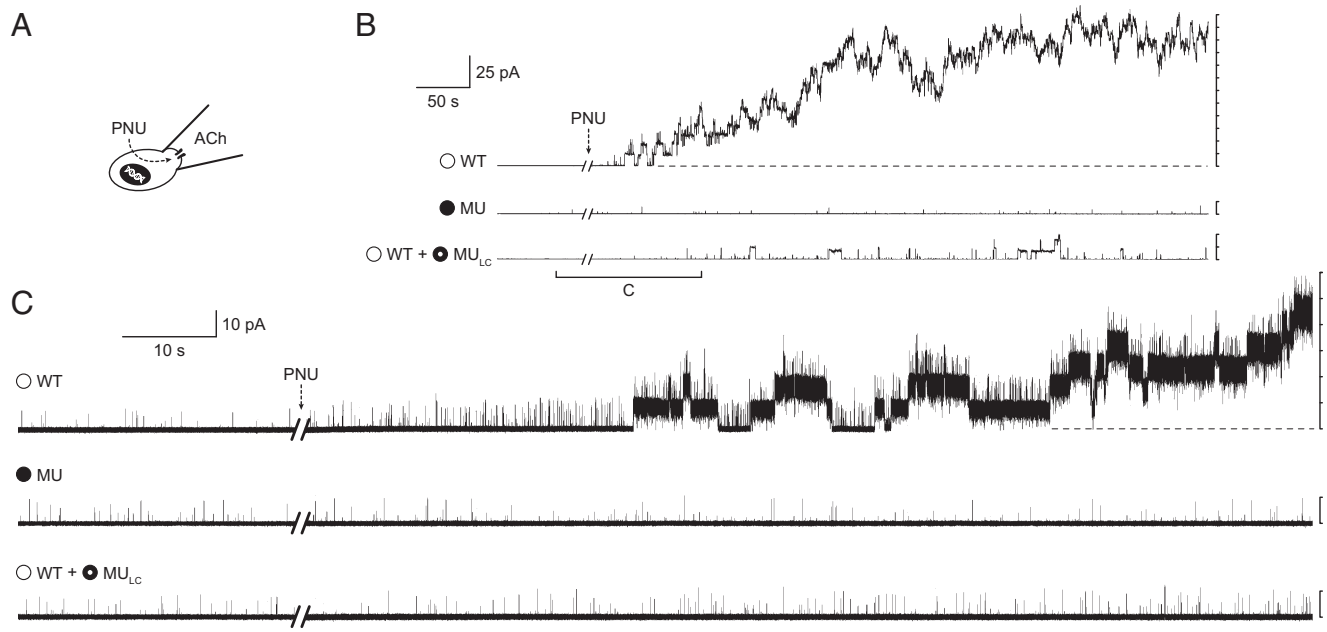

Fig. 3. Mixing wild-type and PNU-resistant subunits leads to receptors that are resistant to PNU. (*A*) Schematic depicting experimental protocol. In each case, 100 μM acetylcholine (ACh) was maintained in the patch pipette, and at the indicated time, PNU was added to the extracellular solution (final PNU concentration = 3 μM). (*B* and *C*) The activity of cell-attached patches before and after PNU addition reveals the PNU potentiation of receptors composed of wild-type subunits (WT; *Upper*), PNU-resistant subunits (MU; *Middle*), and a mixture of wild-type and low-conductance PNU-resistant subunits (WT + MU_{LC}; *Lower*). Despite the activity of the patches being similar before the addition of PNU (*Left*), their activity diverges once PNU is added (*Right*). The data sweeps in (*B*) are filtered at 0.1 kHz, where unpotentiated openings are too brief to be resolved and, instead, prolonged PNU potentiated events dominate the activity. The traces in *C* are expanded views of the bracketed region in *B* and are displayed at a filter frequency of 5 kHz, which better resolves brief unpotentiated openings, thus facilitating comparisons of patch activity before PNU addition. (Scale bars: 10 pA segments.) All recordings were acquired at an applied voltage of −70 mV.

To determine PNU potentiation for each subunit combination, we collected bursts of closely spaced channel openings from each amplitude class and generated a dwell time histogram for each class (Fig. 5 *A* and *B*; *Materials and Methods*). For patches containing receptors with only wild-type α7 subunits, the burst duration histogram is best described by the sum of three exponential components, in which the component with longest mean duration originates exclusively from PNU-potentiated openings. Thus, the fractional area of this third component is a quantitative measure of PNU potentiation. Accordingly, for patches containing receptors with only PNU-resistant subunits, this longest component is absent in the corresponding burst-duration histogram (Fig. 5*B*). These two contrasting burst-duration histograms represent the PNU-sensitive and PNU-resistant baselines with which to compare receptors with different subunit stoichiometry.

Compared with receptors composed solely of wild-type α7 subunits, receptors with a single PNU-resistant subunit show a marked decrease in the fraction of potentiated channel openings (Fig. 5*A*). Substituting a second PNU-resistant subunit essentially eliminates the potentiated openings altogether. Conversely, receptors with one or two wild-type α7 subunits remain insensitive to PNU, similar to receptors composed solely of PNU-resistant subunits (Fig. 5*B*). Thus, PNU potentiation shows a strong dependence on the number of PNU-sensitive subunits (Fig. 5*C*).

Discussion

We used a single-channel electrical fingerprinting strategy (17, 18) to determine the subunit stoichiometry of α7 receptors in which the number of wild-type and PNU-resistant subunits varied. This approach allowed us to simultaneously measure PNU potentiation and the number of intact PNU sites in individual α7 receptors in real-time. Our analysis encompassed receptors with all possible combinations of wild-type and PNU-resistant subunits and allowed us to quantify the contributions of individual subunits to PNU potentiation (Fig. 5*C*). We find that potentiation behaves in a recessive manner: mutating a single PNU site dramatically reduces the appearance of multisecond-long clusters of α7 channel openings, whereas mutating two PNU sites essentially abolishes them. Thus, the most pronounced form of potentiation, the appearance of multisecond-long clusters, requires at least four, if not all five, subunits with intact PNU sites.

Although a change in PNU sensitivity can occur through a change in either PNU affinity or efficacy, the available evidence suggests PNU-resistant subunits have altered PNU affinity. Docking analysis of PNU to a homology model of α7 suggests PNU binds in a cavity framed by transmembrane α-helices within each α7 subunit (16). In accord, the side chains of the substituted residues in the PNU-resistant mutant extend into this cavity and increase the EC_{50} for potentiation ∼30-fold (15). Anesthetics, alcohols, and neurosteroids are thought to bind to a similar location in $GABA_A$ and glycine receptors (21–23), photoactivatable hydrophobic probes label nearby residues in the *Torpedo* acetylcholine receptor (24–26), and X-ray structures of a prokaryotic homolog show anesthetics interacting with residues lining the cavity (27). This intrasubunit site in α7 is distinct from the site for the potentiator ivermectin, which spans transmembrane α-helices from adjacent subunits in the invertebrate Cys-loop receptor, GluCl (28).

Two general mechanisms predict a steep decline of PNU potentiation as the number of subunits with intact PNU sites is reduced. In the first, each subunit contributes an equal increment of energy toward potentiation and the PNU-resistant subunits do not bind PNU. Thus, as the PNU sites are sequentially mutated, potentiation is expected to decrease by a factor of exp(−1), which is close to the observed dependence (Fig. 5*C*). In the second mechanism, potentiation only occurs when all five sites

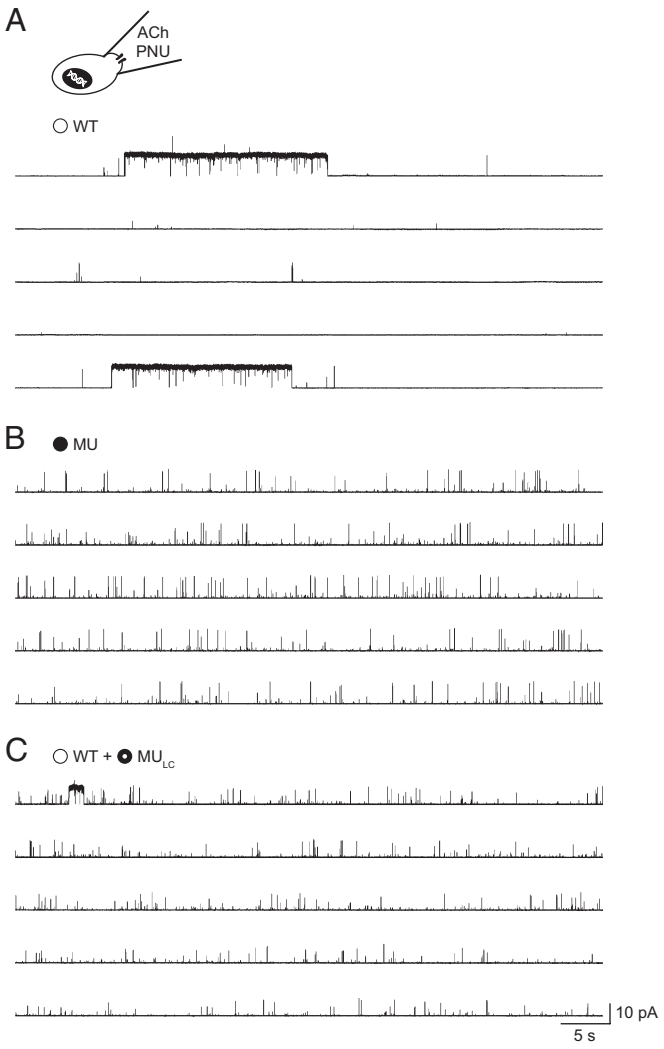

Fig. 4. PNU potentiation at steady state. When both 100 μM acetylcholine (ACh) and 1 μM PNU (PNU) are present in the pipette (inset), cell-attached patches containing receptors with (*A*) only wild-type subunits (WT) exhibit prolonged, PNU-potentiated openings; whereas (*B*) patches containing receptors composed of only PNU-resistant subunits (MU) do not. (*C*) Mixing wild-type subunits with low-conductance PNU-resistant (MU$_{LC}$) subunits leads to receptors with brief, unpotentiated openings. Note that the patch in *A* contains few receptors, whereas the patches in *B* and *C* contain several receptors. In *A*, the presence of prolonged, potentiated openings makes it imperative to limit the number of channels in the patch to prevent excessive overlapping openings (as seen in Fig. 3), whereas in *B* and *C*, the PNU-resistant nature of the receptors makes it beneficial to have a large number of channels in the patch to generate enough brief events for dwell time analysis. All traces are 5-min continuous stretches from individual recordings (i.e., 1 min/sweep). Recordings were made in the cell-attached configuration at an applied voltage of −70 mV. Traces were filtered at 1 kHz.

are occupied by PNU and the PNU-resistant subunits still bind PNU, although with reduced affinity. If PNU binding is noncooperative, potentiation is again expected to decline exponentially, where the steepness of the decline is determined by the relative affinity of the PNU-resistant subunits. The observed dependence would be explained if the PNU-resistant subunits retain ∼40% of the wild-type occupancy at the given PNU concentration (Fig. 5*C*).

Although the simplicity of these mechanisms is appealing, neither scenario fully explains the data. A small but notable departure from the expected relationship is observed for receptors with two mutated PNU sites. Although this stoichiometry is the sole apparent outlier, it was tested in two different ways: with the conductance mutations placed in either the PNU-resistant

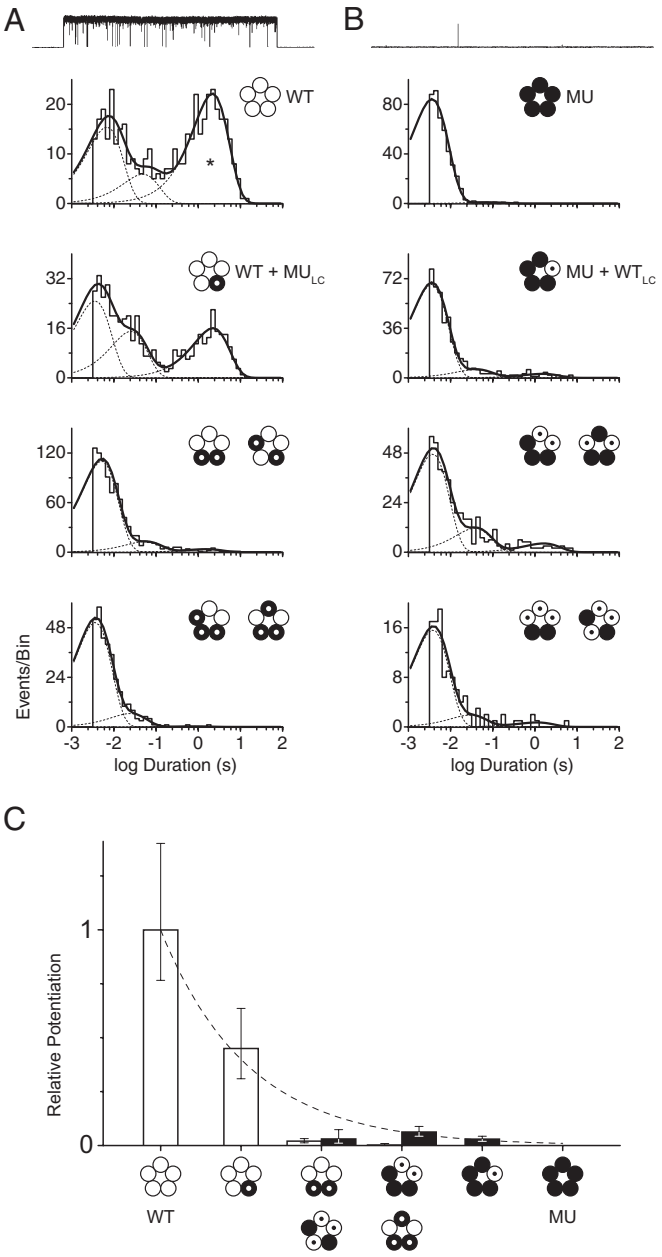

Fig. 5. Subunit-dependent contributions to PNU potentiation in α7. (*A* and *B*) Burst duration histograms (*Materials and Methods*) for α7 receptors containing different numbers of wild-type (WT) and PNU-resistant (MU) subunits, where one of the subunits carries conductance mutations. The component originating from potentiated openings is denoted by the asterisk. The ordinate is plotted on a linear scale to facilitate visual comparisons of the fractional area of the longest component. (*C*) Relative fraction of potentiated openings for each of the subunit combinations, where homopentameric wild-type and PNU-resistant receptors represent potentiated and nonpotentiated baselines, respectively. Bars are colored according to the high-conductance subunit used in the corresponding subunit-mixing experiments (white for WT and black for MU). Note that for the two middle subunit combinations, there are two sets of data from overlapping experiments. The dashed curve in *C* is the overlaid function $y = [0.4]^m$, where m is the number of mutant subunits with a fractional occupancy of 0.4 relative to wild-type subunits. Error bars are 95% confidence intervals of the fits, based on log likelihood ratio tests.

subunit or the wild-type subunit. In both cases, potentiation was less than 4% of maximum, rather than the expected 13.5% (Fig. 5*C*). This suggests that the energetic contributions of the subunits toward potentiation may be unequal or that PNU binding may be cooperative. In either case, cooperative interactions among the subunits would be necessary.

Classical concepts of cooperativity were founded on macroscopic measurements of either ligand occupancy or biological activity as a function of ligand concentration. If the Hill coefficient was greater than one, the system was deemed cooperative (29). Different microscopic interpretations were then envisaged that either postulated interactions between occupied and unoccupied subunits within an oligomer or accorded biological activity to oligomers with a requisite number of ligand-bound subunits (30, 31). In contrast, our approach directly measures the biological activity of every possible partially and fully occupied oligomer and reveals that all but fully occupied oligomers have a muted ability to potentiate. This finding predicts that at a macroscopic level, PNU potentiation is highly cooperative. Thus, our approach illustrates a general single-molecule strategy to assess cooperative mechanisms of biological macromolecules.

The conclusion that as many as five PNU sites are required for full potentiation of α7 is unique, given what is known about pentameric ligand-gated ion channel structure and mechanism. In the best-known example of potentiation, heteropentameric $GABA_A$ receptors are potentiated by benzodiazepines, which bind to a single modulatory site between extracellular regions of the α_1- and γ_2-subunits (32). Furthermore, efficient agonist activation of homopentameric α7/5H-T_3 chimeric receptors requires occupancy of only three of the five agonist sites (17), whereas both heteropentameric $GABA_A$ and muscle-type acetylcholine receptors have only two agonist binding sites to begin with. The different numbers of binding sites required for the action of each ligand indicates divergent mechanisms. Benzodiazepines potentiate agonist responses by modulating activation or preactivation steps (33), whereas agonists themselves are intimately involved in activation. PNU, in contrast, potentiates agonist-induced responses by slowing α7 desensitization (14, 15, 34). Thus, benzodiazepines and agonists modulate "on" responses, whereas PNU modulates the α7 "off" response. In this context, our results have implications for pentameric ligand-gated ion channel desensitization. Although PNU potentiation behaves in a recessive manner, its counterpart, desensitization, behaves in a dominant manner. Only one or two fast desensitizing subunits is enough to dominate the desensitization landscape in α7, and thus the rate of α7 desensitization is governed by its fastest desensitizing subunit. Extrapolating to heteropentameric ligand-gated ion channels, our findings suggest that their desensitization kinetics are determined by the fastest desensitizing subunit.

Materials and Methods

Additional experimental procedures are described in *SI Materials and Methods*.

Expression of Human α7 and Mutants. BOSC 23 cells, modified HEK 293 cells (35), were transfected by calcium phosphate precipitation as described previously (15, 36–38). The PNU-resistant mutant (MU) contains five substitutions within the α7 transmembrane domain (Ser223Thr, Ala226Ser, Met254Leu, Ile281Met, and Val288Ile; Fig. S1) (15), whereas the low-conductance forms of each subunit result from substitution of three arginines into the α7 cytoplasmic domain (Gln428Arg, Glu432Arg, and Ser436Arg; Fig. 2*B*).

Single-Channel Recordings. Recordings were obtained in the cell-attached patch configuration (39) at a membrane potential of −70 mV and at 20°C, as described previously (15, 40, 41). The bath solution contained the following (in mM): 142 KCl, 5.4 NaCl, 1.8 $CaCl_2$, 1.7 $MgCl_2$, and 10 Hepes at pH 7.4. Unless specified otherwise, all pipette solutions contained 100 μM acetylcholine and 1 μM PNU in bath solution with 0.1% (vol/vol) DMSO.

Electrical Fingerprinting. To mitigate any time-dependent effects of PNU, only the first 20 min of each recording were analyzed. Single-channel analysis was performed using the program TAC 4.2.0 (Bruxton), which digitally filters the data (Gaussian response), interpolates the digitized points using a cubic spline function, and detects events using the half-amplitude threshold criterion, as described (42). The differences in open duration between potentiated and nonpotentiated receptors are dramatic and span several orders of magnitude (i.e., minutes vs. milliseconds), which allowed us to filter the data at 1 kHz without loss of pertinent information. This filter setting greatly simplified the amplitude detection and assignment procedure central to the electrical fingerprinting strategy.

To define amplitude classes, the analyses tracked all events regardless of amplitude. For each individual opening, a baseline current, open channel current, and open duration were assigned. For all conditions, openings from between 9 and 16 different recordings were pooled, and event-based amplitude histograms were constructed (Fig. S3). In each case, the different amplitude classes were distinguished and fit by a sum of Gaussian components, where the maxima and width of each component defined the mean ± SD of each amplitude class (Fig. S3).

The electrical fingerprinting strategy works best when the amplitude of channels with a given subunit combination is reproducible and uniform. Therefore, before embarking on subunit-mixing experiments, we defined analysis conditions amenable to both homopentameric wild-type and mutant PNU-resistant receptors. In both cases, the uniformity of event-based amplitude histograms was significantly improved by analyzing openings longer than 3 ms. As a result, all amplitude (and dwell time) histograms include events 3 ms or longer.

Dwell Time Analysis. Openings with amplitudes within 1 SD of the mean amplitude of each class were used to construct dwell time histograms. Because patches containing only high-conductance subunits had a small proportion of low-amplitude events (Fig. S3*A*), "spill over" of these low-amplitude events could have caused misclassification of events in experiments in which both low- and high-conductance subunits were coexpressed. Thus, to avoid spill-over in subunit-mixing experiments, we used subunit ratios that minimized receptors with a greater number of high-conductance subunits than desired and did not analyze recordings if they contained events from such receptors. For example, the dwell time histogram for the 4WT:1MU_{LC} subunit combination was generated from patches in which events from receptors with five WT subunits were absent (i.e., only the events from patches with four high-conductance subunits or less were pooled). Likewise, the histogram for the 3WT:2MU_{LC} combination was generated from patches in which events from receptors with four or five WT subunits were absent. A consequence of these stringent selection criteria is that fewer recordings are pooled for each analysis as the number of high-conductance subunits decreases, which in turn gives rise to dwell time histograms with fewer and fewer events (e.g., Fig. 5*B*). For this reason, we have restricted our analysis to subunit combinations with two or more high-conductance subunits.

Potentiated channels were defined by the presence of non-desensitizing episodes in which several openings occurred in quick succession (i.e., bursts of openings). The presented dwell time histograms are burst-duration histograms (43) in which consecutive openings separated by intervening closings briefer than a defined critical time (τ_{crit} = 2 ms throughout) have been combined into single bursts. Burst durations were plotted using a logarithmic abscissa and a linear ordinate. The linear ordinate facilitates comparisons of component proportions between histograms (Fig. 5 *A* and *B*).

The sum of exponentials was fitted to the dwell times by maximum likelihood using the programs TACfit 4.2.0 (Bruxton) and R (The R Foundation for Statistical Computing) (44). The relative proportion of openings occurring in nondesensitizing episodes (i.e., the fractional area under the longest/third component) reflects PNU potentiation of the channels (15). For the bar graph in Fig. 5*C*, the fraction of openings in this longest/third component was normalized to the proportion of openings in the briefest/first component. For patches containing only wild-type subunits, this normalized fraction was used as an upper limit of potentiation (i.e., 1), whereas for patches containing only PNU-resistant subunits this fraction was a lower limit (i.e., 0). The error bars in Fig. 5 represent 95% confidence intervals of the fits, as determined from log likelihood ratio tests performed with the statistical program R.

ACKNOWLEDGMENTS. We thank Chris R. Free for mutagenesis and Dr. Terry Therneau for assistance with "R." This work was supported by National Institutes of Health Grant NS031744 (to S.M.S.) and by a Canadian Institutes of Health Research Fellowship (to C.J.B.D.).

1. Overington JP, Al-Lazikani B, Hopkins AL (2006) How many drug targets are there? *Nat Rev Drug Discov* 5(12):993–996.
2. Hille B (2001) *Ion Channels of Excitable Membranes* (Sinauer Associates, Sunderland, MA), 3rd Ed.
3. Corringer P-J, et al. (2012) Structure and pharmacology of pentameric receptor channels: from bacteria to brain. *Structure* 20(6):941–956.
4. Sine SM, Engel AG (2006) Recent advances in Cys-loop receptor structure and function. *Nature* 440(7083):448–455.
5. Couturier S, et al. (1990) A neuronal nicotinic acetylcholine receptor subunit (α7) is developmentally regulated and forms a homo-oligomeric channel blocked by α-BTX. *Neuron* 5(6):847–856.
6. Chang KT, Berg DK (1999) Nicotinic acetylcholine receptors containing α7 subunits are required for reliable synaptic transmission in situ. *J Neurosci* 19(10):3701–3710.
7. Freedman R, et al. (1997) Linkage of a neurophysiological deficit in schizophrenia to a chromosome 15 locus. *Proc Natl Acad Sci USA* 94(2):587–592.
8. Freedman R, Hall M, Adler LE, Leonard S (1995) Evidence in postmortem brain tissue for decreased numbers of hippocampal nicotinic receptors in schizophrenia. *Biol Psychiatry* 38(1):22–33.
9. Qi X-L, Nordberg A, Xiu J, Guan Z-Z (2007) The consequences of reducing expression of the α7 nicotinic receptor by RNA interference and of stimulating its activity with an α7 agonist in SH-SY5Y cells indicate that this receptor plays a neuroprotective role in connection with the pathogenesis of Alzheimer's disease. *Neurochem Int* 51(6-7): 377–383.
10. Hajós M, Rogers BN (2010) Targeting α7 nicotinic acetylcholine receptors in the treatment of schizophrenia. *Curr Pharm Des* 16(5):538–554.
11. Leiser SC, Bowlby MR, Comery TA, Dunlop J (2009) A cog in cognition: how the α7 nicotinic acetylcholine receptor is geared towards improving cognitive deficits. *Pharmacol Ther* 122(3):302–311.
12. Taly A, Corringer P-J, Guedin D, Lestage P, Changeux J-P (2009) Nicotinic receptors: allosteric transitions and therapeutic targets in the nervous system. *Nat Rev Drug Discov* 8(9):733–750.
13. Haydar SN, Dunlop J (2010) Neuronal nicotinic acetylcholine receptors - targets for the development of drugs to treat cognitive impairment associated with schizophrenia and Alzheimer's disease. *Curr Top Med Chem* 10(2):144–152.
14. Hurst RS, et al. (2005) A novel positive allosteric modulator of the α7 neuronal nicotinic acetylcholine receptor: in vitro and in vivo characterization. *J Neurosci* 25(17): 4396–4405.
15. daCosta CJB, Free CR, Corradi J, Bouzat C, Sine SM (2011) Single-channel and structural foundations of neuronal α7 acetylcholine receptor potentiation. *J Neurosci* 31(39):13870–13879.
16. Young GT, Zwart R, Walker AS, Sher E, Millar NS (2008) Potentiation of α7 nicotinic acetylcholine receptors via an allosteric transmembrane site. *Proc Natl Acad Sci USA* 105(38):14686–14691.
17. Rayes D, De Rosa MJ, Sine SM, Bouzat C (2009) Number and locations of agonist binding sites required to activate homomeric Cys-loop receptors. *J Neurosci* 29(18): 6022–6032.
18. Andersen N, Corradi J, Bartos M, Sine SM, Bouzat C (2011) Functional relationships between agonist binding sites and coupling regions of homomeric Cys-loop receptors. *J Neurosci* 31(10):3662–3669.
19. Unwin N (2005) Refined structure of the nicotinic acetylcholine receptor at 4A resolution. *J Mol Biol* 346(4):967–989.
20. Kelley SP, Dunlop JI, Kirkness EF, Lambert JJ, Peters JA (2003) A cytoplasmic region determines single-channel conductance in 5-HT3 receptors. *Nature* 424(6946): 321–324.
21. Belelli D, Lambert JJ, Peters JA, Wafford K, Whiting PJ (1997) The interaction of the general anesthetic etomidate with the gamma-aminobutyric acid type A receptor is influenced by a single amino acid. *Proc Natl Acad Sci USA* 94(20):11031–11036.
22. Mihic SJ, et al. (1997) Sites of alcohol and volatile anaesthetic action on GABA(A) and glycine receptors. *Nature* 389(6649):385–389.
23. Hosie AM, Wilkins ME, da Silva HMA, Smart TG (2006) Endogenous neurosteroids regulate GABAA receptors through two discrete transmembrane sites. *Nature* 444 (7118):486–489.
24. Arevalo E, Chiara DC, Forman SA, Cohen JB, Miller KW (2005) Gating-enhanced accessibility of hydrophobic sites within the transmembrane region of the nicotinic acetylcholine receptor's δ-subunit. A time-resolved photolabeling study. *J Biol Chem* 280(14):13631–13640.
25. Garcia G, 3rd, et al. (2007) [^{3}H]Benzophenone photolabeling identifies state-dependent changes in nicotinic acetylcholine receptor structure. *Biochemistry* 46(36): 10296–10307.
26. Hamouda AK, Stewart DS, Husain SS, Cohen JB (2011) Multiple transmembrane binding sites for p-trifluoromethyldiazirinyl-etomidate, a photoreactive Torpedo nicotinic acetylcholine receptor allosteric inhibitor. *J Biol Chem* 286(23):20466–20477.
27. Nury H, et al. (2011) X-ray structures of general anaesthetics bound to a pentameric ligand-gated ion channel. *Nature* 469(7330):428–431.
28. Hibbs RE, Gouaux E (2011) Principles of activation and permeation in an anion-selective Cys-loop receptor. *Nature* 474(7349):54–60.
29. Brown W, Hill A (1923) The oxygen-dissociation curve of blood, and its thermodynamical basis. *Proc Biol Sci* 94:297–334.
30. Monod J, Wyman J, Changeux J-P (1965) On the nature of allosteric transitions: a plausible model. *J Mol Biol* 12:88–118.
31. Koshland DE, Jr., Némethy G, Filmer D (1966) Comparison of experimental binding data and theoretical models in proteins containing subunits. *Biochemistry* 5(1): 365–385.
32. Sigel E (2002) Mapping of the benzodiazepine recognition site on GABA(A) receptors. *Curr Top Med Chem* 2(8):833–839.
33. Gielen MC, Lumb MJ, Smart TG (2012) Benzodiazepines modulate GABAA receptors by regulating the preactivation step after GABA binding. *J Neurosci* 32(17): 5707–5715.
34. Williams DK, Wang J, Papke RL (2011) Investigation of the molecular mechanism of the α7 nicotinic acetylcholine receptor positive allosteric modulator PNU-120596 provides evidence for two distinct desensitized states. *Mol Pharmacol* 80(6): 1013–1032.
35. Pear WS, Nolan GP, Scott ML, Baltimore D (1993) Production of high-titer helper-free retroviruses by transient transfection. *Proc Natl Acad Sci USA* 90(18):8392–8396.
36. Sine SM (1993) Molecular dissection of subunit interfaces in the acetylcholine receptor: identification of residues that determine curare selectivity. *Proc Natl Acad Sci USA* 90(20):9436–9440.
37. Bouzat C, Bren N, Sine SM (1994) Structural basis of the different gating kinetics of fetal and adult acetylcholine receptors. *Neuron* 13(6):1395–1402.
38. Sine SM, Quiram P, Papanikolaou F, Kreienkamp HJ, Taylor P (1994) Conserved tyrosines in the α subunit of the nicotinic acetylcholine receptor stabilize quaternary ammonium groups of agonists and curariform antagonists. *J Biol Chem* 269(12): 8808–8816.
39. Hamill OP, Marty A, Neher E, Sakmann B, Sigworth FJ (1981) Improved patch-clamp techniques for high-resolution current recording from cells and cell-free membrane patches. *Pflugers Arch* 391(2):85–100.
40. Bouzat C, Bartos M, Corradi J, Sine SM (2008) The interface between extracellular and transmembrane domains of homomeric Cys-loop receptors governs open-channel lifetime and rate of desensitization. *J Neurosci* 28(31):7808–7819.
41. Rayes D, Spitzmaul G, Sine SM, Bouzat C (2005) Single-channel kinetic analysis of chimeric α7-5HT3$_A$ receptors. *Mol Pharmacol* 68(5):1475–1483.
42. Colquhoun D, Sigworth FJ (1983) in Fitting and statistical analysis of single-channel records. *Single Channel Recording*, eds Sakmann B, Neher E (Plenum Press, New York), pp 191–264.
43. Colquhoun D, Hawkes AG (1982) On the stochastic properties of bursts of single ion channel openings and of clusters of bursts. *Philos Trans R Soc Lond B Biol Sci* 300(1098):1–59.
44. R Development Core Team (2012) R: A language and environment for statistical computing (R Foundation for Statistical Computing, Vienna, Austria). Available at http://www.R-project.org/. Last accessed June 11, 2012.